Method for Computing the Anisotropy of the Solid-Liquid Interfacial Free Energy

J. J. Hoyt,[1] Mark Asta,[2] and Alain Karma[3]

[1]*Sandia National Laboratories, MS 9161, P.O. Box 969, Livermore, California 94550*

[2]*Department of Materials Science and Engineering, Northwestern University, Evanston, Illinois, 60208*

[3]*Physics Department, Northeastern University, Boston, Massachusetts 02115*

(Received 31 August 2000)

We present a method to compute accurately the weak anisotropy of the solid-liquid interfacial free energy, a parameter which influences dendritic evolution in materials with atomically rough interfaces. The method is based on monitoring interfacial fluctuations during molecular dynamics simulation and extracting the interfacial stiffness which is an order of magnitude more anisotropic than the interfacial free energy. We present results for pure Ni with interatomic potentials derived from the embedded atom method.

DOI: 10.1103/PhysRevLett.86.5530 PACS numbers: 68.08.–p, 64.70.Dv, 81.30.Fb

The formation of dendrites during the solidification of a liquid is an important process from both technological and scientific points of view [1]. The mechanical integrity of a cast, brazed, or soldered alloy depends critically on the complex morphologies which appear during solidification. In addition, dendrite formation represents a rather striking example of spontaneous pattern formation in a nonequilibrium system, a phenomenon studied extensively in many areas of physics, chemistry, and biology.

Numerous studies over the last two decades have convincingly demonstrated that crystalline anisotropy plays a crucial role in dendritic solidification [1]. Dynamically, its main role is to prevent the growing tips of primary and higher order dendrite branches from splitting continuously, thereby guiding morphological development into a branched pattern that reflects on a macroscopic scale the underlying atomic symmetry of the crystal. Moreover, the dendrite growth rate depends sensitively on the strength of crystalline anisotropy as predicted by microscopic solvability theory [2] and recently validated by phase-field simulations in three dimensions [3]. Despite this progress, closure between theory and experiment has remained a major problem. A main obstacle is that the anisotropy of the solid-liquid interfacial energy is characteristically very weak for dendrite forming systems with low entropy of melting and atomically rough interfaces. Thus, the precise value of this key parameter controlling microstructural evolution has so far remained too difficult to compute or measure experimentally for metallic systems of practical relevance, and existing anisotropy measurements remain limited to a few transparent organic systems [4].

The purpose of this Letter is to describe a computational method that can predict accurately the weak anisotropy of the interfacial free energy with the level of accuracy needed to model accurately microstructural evolution in solidification and other pattern forming systems. The method is presented here for the concrete example of the crystal-melt interface in pure Ni where the interatomic potential is modeled using the embedded atom method (EAM) [5,6]. However, it should also be applicable to compute the excess free energy of the interface between various liquid crystalline phases, and notably the nematic-isotropic interface [7]. Moreover, this method provides an accurate prediction of the interfacial free energy even when the latter is isotropic, which is directly relevant for a wide range of hydrodynamic problems. We summarize here the essential ingredients of the method and a more detailed extension to compute interfacial kinetic properties will be given elsewhere.

For weakly anisotropic crystals with an underlying cubic symmetry, the anisotropy parameter has been traditionally defined [2,3] by examining the variation of the interfacial energy, γ, with the angle θ between the [100] direction and the direction normal to the interface that lies in the (001) plane, or to lowest order

$$\gamma(\theta) = \gamma_0(1 + \epsilon \cos 4\theta + \ldots), \tag{1}$$

where ϵ is typically small ($\sim$0.01). For the transparent organic crystals used in fundamental studies of dendritic growth, it has been possible to measure ϵ [4] by imaging the two-dimensional (2D) projection of the 3D equilibrium crystal shape along the [001] direction. In an atomistic simulation, however, such a measurement is not feasible because the shape fluctuations of a small crystal are too large, even with a million atoms. Another possibility is to compute γ for a flat interface for different orientations. However, the uncertainty in γ for each orientation must be much smaller than ϵ, a task that would require unreasonably long averaging times in simulations. For example, Broughton and Gilmer [8] computed the crystal-melt interfacial energy in a Lennard-Jones system using molecular dynamics (MD) and quoted a 7% uncertainty in γ which is too high to extract ϵ. Analytic descriptions of the crystal-melt interface based on density functional theory [9] offer the possibility of computing γ [10]. However, such theoretical approaches have been limited thus far to simple hard and soft sphere systems.

We circumvent the above difficulties by computing, instead of γ, the interfacial stiffness, $\gamma + \gamma''$, where we

 0031-9007/01/86(24)/5530(4)$15.00

have defined $\gamma'' \equiv d^2\gamma/d\theta^2$. The key point is that this quantity, which enters directly the Gibbs-Thomson condition of standard solidification models, is an order of magnitude more anisotropic than γ itself, i.e., for γ given by Eq. (1), $\gamma + \gamma'' = \gamma_0(1 - \alpha\cos 4\theta)$, with $\alpha = 15\epsilon$. Thus, in general, the stiffness anisotropy is much easier to compute accurately by MD simulations than the corresponding one for γ, and the two anisotropies can always be related. This remains true even for higher order forms of γ than Eq. (1), as we see below. To obtain the stiffness for a given orientation, we use the known fact that this quantity can be related to the spectrum of interfacial fluctuations in thermodynamic equilibrium [11]. To see how this relationship comes about in the form appropriate for our simulations, consider a thin slab that is infinite along the vertical y axis, of width W along the x axis, and of thickness $b \ll W$ along the z axis. Furthermore, let $h(x)$ denote the height (y coordinate) of the fluctuating ribbonlike interface that separates the solid and liquid phases in this slab. We focus on this geometry because it gives rise to larger amplitude fluctuations than a bulk 3D system containing a 2D square interface. Namely, the mean square height of the interface, $\langle h^2\rangle$, scales proportionally to W in the former, but only as $\ln W$ in the latter [12]. For the slab, the ribbonlike interface shape can be written as a sum of Fourier modes: $h(x) = \sum_k A(k)\exp(ikx)$. A relation between the interface stiffness and the mean square amplitude $\langle|A(k)|^2\rangle$ can then be obtained by noting that the mean energy, E_k, in each Fourier mode must be equal to $k_B T_M$ (i.e., 2 degrees of freedom per mode corresponding to $\sin(kx)$ and $\cos(kx)$, where k_B is the Boltzmann constant and T_M is the equilibrium melting temperature) which follows from equipartition of energy. Using the expression for the interfacial energy, $b\int ds\,\gamma(\theta)$, where $ds \approx 1 + (dh/dx)^2/2$ is the element of arclength along the ribbon and $\theta \approx dh/dx$ is the angle between the interface normal and the y axis, we obtain at once the desired relation

$$\langle|A(k)|^2\rangle = \frac{k_B T_M}{bW(\gamma + \gamma'')k^2}, \qquad (2)$$

which allows us to extract the stiffness from our MD simulations, i.e., by measuring the slope of the straight line that fits $1/\langle|A(k)|^2\rangle$ plotted vs k^2. Note that γ'' in the denominator of Eq. (2) originates from the energy cost of bending locally the interface away from its macroscopic orientation, which is why the fluctuation spectrum measures directly the stiffness.

The next question that needs to be addressed is how many independent stiffness measurements (for different orientations) are needed to parametrize γ? Let us denote by $\hat{x}_1$, $\hat{x}_2$, and $\hat{x}_3$ the unit vectors parallel to the [100], [010], and [001] directions, respectively, and by n_i ($i \in [1,3]$) the components of the interface normal, $\hat{n}$, in the (x_1, x_2, x_3) coordinate system. For a weakly anisotropic crystal, $\gamma(\hat{n})$ can be expanded in terms of "Kubic harmonics" [13], which is a linear combination of spherical harmonics that obey a cubic symmetry:

$$\gamma(\hat{n})/\gamma_o = 1 - 3\epsilon + 4\epsilon\sum_{i=1}^{3} n_i^4 + \delta\left(\sum_{i=1}^{3} n_i^6 + 30 n_1^2 n_2^2 n_3^2\right) + \ldots. \qquad (3)$$

Consider a simulation in which the 100 face of the crystal is adjacent to the liquid phase and the [010] direction runs parallel to the 1D interface. For brevity of notation, we denote this orientation by 100 [010]. [The coordinate system for this orientation is illustrated in Fig. 1(b).] This corresponds, equivalently, to the choice of unit vectors $\hat{x} = \hat{x}_2$ and $\hat{y} = \hat{x}_1$, where recall that $\hat{x}$ is parallel to the 1D interface and $\hat{y}$ is normal to the crystal face. Similarly, for 110 $[1\bar{1}0]$, we have $\hat{x} = (\hat{x}_1 - \hat{x}_2)/\sqrt{2}$ and $\hat{y} = (\hat{x}_1 + \hat{x}_2)/\sqrt{2}$, and so forth for other orientations. Since the interface fluctuates in the (x, y) plane and θ is the angle between $\hat{n}$ and $\hat{y}$, the stiffness for a given choice of slab orientation $(\hat{x}, \hat{y})$ is simply obtained by substituting the expression $n_i = (\cos\theta\hat{y} + \sin\theta\hat{x})\cdot\hat{x}_i$ into Eq. (3) for $i \in [1,3]$, in which case γ becomes only a function of θ. The stiffness is then $\gamma + d^2\gamma/d\theta^2$ evaluated at $\theta = 0$. Results of this procedure are reported for five different orientations in the middle column of Table I. For $\delta = 0$,

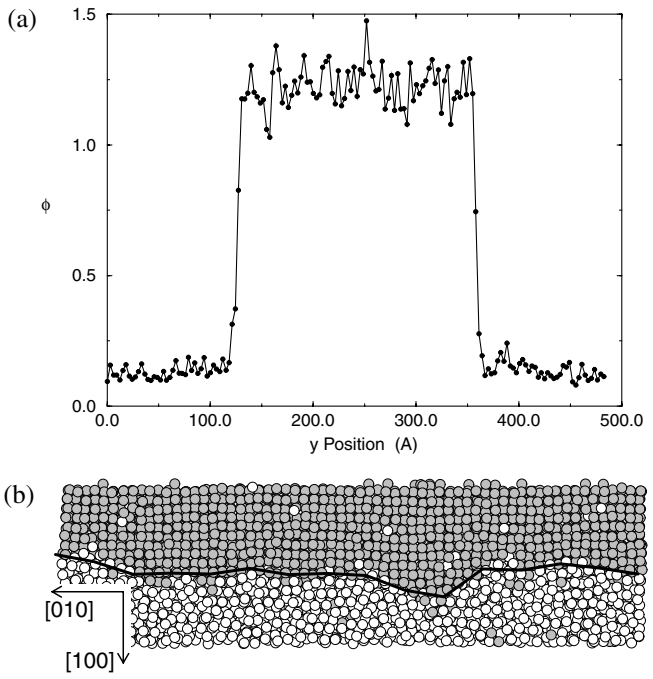

FIG. 1. (a) Plot of the order parameter ϕ vs y at a point along the interface. Results were obtained from a single configuration during an MD simulation. (b) Portion of the solid-liquid interface obtained from one snapshot of an MD simulation for the 100 [010] orientation (the thin direction, i.e., 001, points into the page). Atoms are shaded based on the value of the order parameter ϕ defined in the text. Superimposed as a thick line is the interface position corresponding to the $\phi \approx 0.7$ contour.

TABLE I. Stiffness for different orientations computed analytically using Eq. (3) (middle column) and by linear fits of $1/\langle|A(k)|^2\rangle bW$ vs k^2 in MD simulations (right column).

Orientation	$(\gamma + \gamma'')/\gamma_0$	$\gamma + \gamma''$ (mJ/m^2)
100 [010]	$1 - 15\epsilon - 5\delta$	234
110 [1$\bar{1}$0]	$1 + 15\epsilon + (25/4)\delta$	413
110 [001]	$1 + 9\epsilon + (55/4)\delta$	207
100 [012]	$1 + (387/25)\epsilon + (114/25)\delta$	192
110 [1$\bar{1}$2]	$1 + \epsilon + (45/4)\delta$	277

Eq. (3) reduces to the lowest order form of anisotropy used in theoretical studies of dendritic growth to date, and to Eq. (1) in a 2D cross section. For this choice, only two independent stiffness measurements are needed to determine γ_0 and ϵ independently. We first determined these two quantities in Ni by using the two stiffness measurements reported in the first two rows of Table I, but found that the measured stiffness of the third row could not be fitted accurately. Consequently, we determined γ_0, ϵ, and δ, from the stiffness measurements of the first three rows, and then checked that the stiffness of rows 4 and 5 were accurately reproduced. In general, as many independent stiffness measurements are needed as independent parameters in the cubic harmonic expansion of Eq. (3), plus a few more to check convergence.

Let us now briefly describe the MD simulations and the results. Interatomic potentials for Ni were modeled with the embedded atom method. The EAM is a semiempirical technique which includes multibody atomic interations [5] and which has been proven to be very successful in reproducing various structural, thermodynamic, and dynamic properties of late transition and noble metals [6]. Here, the Ni potential originally developed by Foiles, Baskes, and Daw [14] has been employed and other versions of the EAM Ni potential will be investigated elsewhere. MD simulations were performed in the thin slab geometry introduced above, with periodic boundary conditions on all sides. The slab width W was chosen on the order of 250 Å, with W varying somewhat with crystal orientation. Because of the periodic boundary conditions, two solid-liquid interfaces perpendicular to the y direction are contained in each slab. Therefore, in order to avoid entropic interactions between the two interfaces as much as possible, the slab height along the y direction was chosen to be $2W$. Finally, the slab thickness along the z direction was taken to be as small as possible, yet greater than the range of interaction of the EAM potential (e.g., three unit cells for $z = [001]$). A typical simulation contained 100 000–150 000 atoms. MD runs were carried out in the microcanonical ensemble, and separate runs at constant T and P yielded identical fluctuation spectra $\langle|A(k)|^2\rangle$. The equations of motion were solved with a time step of 2 fs and equilibration of the solid-liquid system at the melting point required 60 ps runs. Subsequently, snapshots of the interface position were collected every 100 time steps for a total of 1250 configurations (125 ps). Locating the position of the solid-liquid interface requires a means of labeling an atom in the simulation as belonging to either the liquid or solid phase. Although several schemes have been developed for this purpose [15–17], we have found the most accurate to be the following. For any of the 12 nearest neighbors of a given atom one can compute the distance the neighbor makes from the ideal fcc positions of the crystal in the given orientation (denoted by $\vec{r}_{\rm fcc}$), which just requires a knowledge of the lattice parameter at the melting temperature and the crystal orientation. The sum of the distances over the 12 neighbors, $\phi = \frac{1}{12}\sum_i |\vec{r}_i - \vec{r}_{\rm fcc}|^2$, acts as an "order parameter" for the central atom. The x direction in the simulation cell is divided into several slices and the order parameter averaged over the slice is computed as a function of the distance y. As the solid-liquid interface is traversed, ϕ changes very abruptly as shown in Fig. 1(a), such that the interface can be accurately located as illustrated in Fig. 1(b). Specifically, the interface was found by the contour defined by $\phi = 0.7$.

Figure 2 shows the fluctuation spectra, $\langle|A(k)|^2\rangle$ vs k, on a log-log scale for the first three orientations in Table I. Standard deviations for the quantity $\langle|A(k)|^2\rangle$ were found to be on the order of the size of the data points in Fig. 2. The solid lines in the figure represent slopes of -2, consistent with the prediction of Eq. (2). It is clear that over a wide range of k, the correct wave number dependence is observed. For all orientations, we observe a leveling off at small k which is most likely due to the aforementioned entropic repulsion between the two solid-liquid interfaces. The fact that the three curves of Fig. 2 are offset from one another is a direct consequence of the stiffness anisotropy.

The anisotropy can be more easily seen in Fig. 3 that plots the reciprocal of the fluctuation spectra times bW vs k^2. According to Eq. (2), the slope of the lines in Fig. 3 is proportional to the stiffness for the stated orientation.

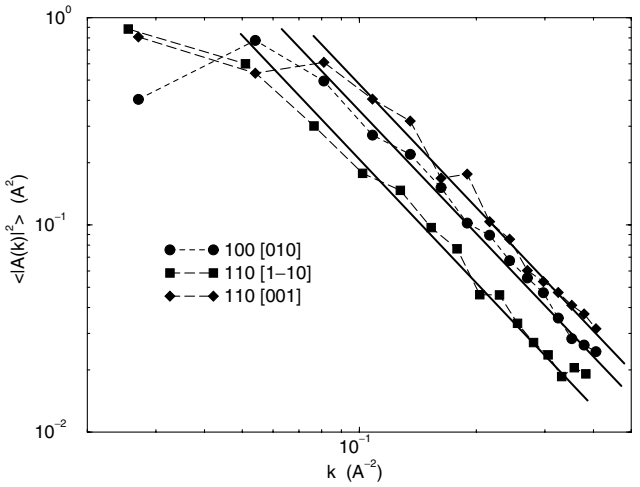

FIG. 2. Log-log plot of the fluctuation spectra, $\langle|A(k)|^2\rangle$ vs k, for pure Ni in three crystal orientations. The solid lines indicate a slope of k^{-2}.

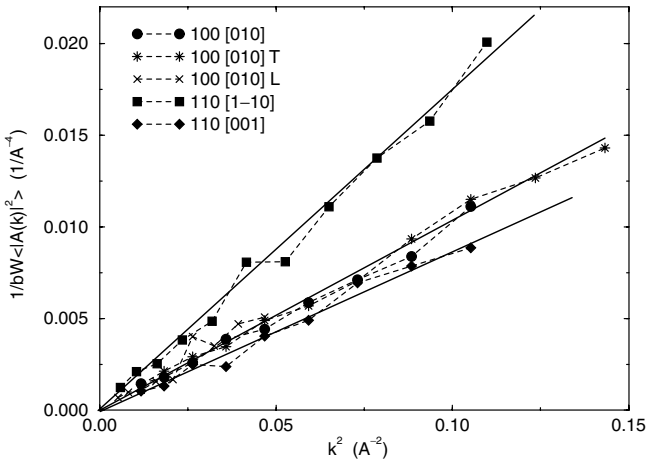

FIG. 3. $1/\langle|A(k)|^2\rangle bW$ vs k^2 for three crystal orientations. The slope of the lines is proportional to the solid-liquid interface stiffness and a clear anisotropy is observed. Also shown are results for different size simulation cells for the 100 interface (see text).

Also shown in the figure is an examination of the system size dependence of the simulations. The 100 run labeled T refers to a simulation cell which is 25% thicker (four unit cells in the z direction rather than three) and the run denoted L corresponds to a simulation in which the slab width was 50% larger. The overlap of all three 100 data sets confirms that the simulations are converged with respect to the slab dimension. The least squares fits of the 100 [010], 110 $[1\bar{1}0]$, and 110 [001] fluctuation data yield the stiffness values reported in the first three rows of the right column in Table I, which by comparison with the analytical expressions of the middle column uniquely sets $\gamma_o = 325.88\ \mathrm{mJ/m^2}$, $\epsilon = 0.022\,69$, and $\delta = -0.011\,68$. Using these values, the analytically predicted values of the stiffness for the 100 [012] and 110 $[1\bar{1}2]$ directions (bottom two rows of middle column of Table I) are then 194 and 276 (in $\mathrm{mJ/m^2}$). These values are in good agreement with the values extracted from the MD simulations (bottom two rows of right column of Table I), which indicates that the anisotropy form of Eq. (3) can reproduce fairly accurately the interfacial free energy for any given orientation. A comparison of the isotropic part of this energy (γ_0) with various empirical estimates will be given elsewhere.

In summary, the very small anisotropy in the solid-liquid interfacial free energy can be found by monitoring the fluctuations of the interface position during molecular dynamics simulations. The success of the technique stems from the fact that it is the stiffness, not the interfacial energy alone, that controls the fluctuation spectra and the stiffness can vary significantly as a function of orientation.

We thank Dr. V. Ozoliņš for many helpful discussions and pointing out the correct form of the Kubic expansion and Jean Bragard for his help in preparing Table I. This research was supported by the U.S. Department of Energy, Office of Basic Energy Sciences, Materials Science Division, under Contracts No. DE-AC04-94AL85000 and No. DE-FG02-92ER45471, as well as the DOE Computational Materials Science Network program.

Note added in proof.—During preparation of this manuscript we became aware of the computations of the solid-liquid interfacial free energy in the hard sphere system using a cleaving technique [18].

[1] For a recent review, see W. J. Boettinger, S. R. Coriell, A. L. Greer, A. Karma, W. Kurz, M. Rappaz, and R. Trivedi, Acta Mater. **48**, 43 (2000).

[2] J. S. Langer in *Chance and Matter,* Proceedings of the Les Houches Summer School, Session XLVI, edited by J. Souletie, J. Vannimenus, and R. Stora (North-Holland, Amsterdam, 1987), pp. 629–711; D. Kessler, J. Koplik, and H. Levine, Adv. Phys. **37**, 255 (1988).

[3] A. Karma and W-J. Rappel, Phys. Rev. Lett. **77**, 4050 (1996); Phys. Rev. E **57**, 4323 (1998).

[4] M. E. Glicksman and N. B. Singh, J. Cryst. Growth **98**, 277 (1989); M. Muschol, D. Liu, and H. Z. Cummins, Phys. Rev. A **46**, 1038 (1992).

[5] M. S. Daw and M. I. Baskes, Phys. Rev. Lett. **50**, 1285 (1983); Phys. Rev. B **29**, 6443 (1984).

[6] M. S. Daw, S. M. Foiles, and M. I. Baskes, Mater. Sci. Rep. **9**, 251 (1993).

[7] P. Oswald, J. Bechhoefer, and A. Libchaber, Phys. Rev. Lett. **58**, 2318 (1987).

[8] J. Q. Broughton and G. H. Gilmer, J. Chem. Phys. **84**, 5759 (1986).

[9] H. Lowen, Phys. Rep. **237**, 249 (1994); B. B. Laird and A. D. J. Haymet, Chem. Rev. **92**, 1819 (1992).

[10] W. A. Curtin and N. W. Ashcroft, Phys. Rev. A **32**, 2909 (1985); A. R. Denton and N. W. Ashcroft, Phys. Rev. A **39**, 4701 (1989); N. Choudhury and S. K. Ghosh, Phys. Rev. E **57**, 1939 (1998).

[11] M. P. A. Fisher, D. S. Fisher, and J. D. Weeks, Phys. Rev. Lett. **48**, 368 (1982).

[12] A. Karma, Phys. Rev. Lett. **70**, 3439 (1993); Phys. Rev. E **48**, 3441 (1993).

[13] A. L. Altman and A. P. Cracknell, Rev. Mod. Phys. **37**, 19 (1965).

[14] S. M. Foiles, M. I. Baskes, and M. S. Daw, Phys. Rev. B **33**, 7983 (1986).

[15] P. J. Steinhardt, D. R. Nelson, and M. Ronchetti, Phys. Rev. B **28**, 784 (1983).

[16] O. Rodriguez de la Fuente and J. M. Soler, Phys. Rev. Lett. **81**, 3159 (1998).

[17] W. J. Briels and H. L. Tepper, Phys. Rev. Lett. **79**, 5074 (1997).

[18] R. L. Davidchack and B. B. Laird, Phys. Rev. Lett. **85**, 4751 (2000).